Hindawi
Mathematical Problems in Engineering
Volume 2019, Article ID 8650243, 14 pages
https://doi.org/10.1155/2019/8650243

Research Article

Fuzzy Iterative Sliding Mode Control Applied for Path Following of an Autonomous Underwater Vehicle with Large Inertia

Guanxue Wang, Guohua Xu, Gang Liu, Wenjin Wang, and Ben Li

School of Naval Architecture and Ocean Engineering, Huazhong University of Science and Technology, Wuhan 430074, China

Correspondence should be addressed to Guohua Xu; hustxu@vip.sina.com

Received 20 September 2018; Revised 28 November 2018; Accepted 27 December 2018; Published 10 January 2019

Guest Editor: Gerhard-Wilhelm Weber

The aim of this paper is to develop a fuzzy iterative sliding mode control (FISMC) scheme for special autonomous underwater vehicles (AUVs) on three-dimensional (3D) path following. In this paper, the characteristics of the AUV are considered, which include a large scale, large inertia, and high speed. The FISMC controller designs iterative sliding mode surfaces by using a hyperbolic tangent function to keep the system with fast convergence and robust performance. At the same time, system uncertainties and environmental disturbances are taken into account. The control algorithm introduces fuzzy control to optimize the control parameters online to enhance the adaptability of the system and inhibit the chattering of the actuators. The performance of the proposed FISMC is demonstrated with numerical simulations.

1. Introduction

In the last decades, AUVs have attracted more and more attention for their multifunctions and practicability in many fields. They have been used in exploring resources, graphic mapping, underwater pipelines inspection, seabed surface reconstruction, and so on [1–3]. Due to the uncertainty and complexity of a marine environment, it is necessary to improve the performance of the AUV, especially for 3D path following, in which the robustness and adaptability of the vehicles are the most important.

Before choosing a reliable control scheme, it is essential to comprehend the features of the AUV. Firstly, a traditional AUV is an underactuated and second-order nonholonomic system [4]. At the same time, the AUV's rudder and propeller have range and frequency saturation. This causes that the real time of the controller will decrease. Also, considering the wave and current, this requires the system to be antidisturbance [5–7]. All of these characteristics bring more challenges to controlling the AUV [8, 9].

Various researches have been carried out for AUVs' control, such as adaptive control, suboptimal control, backstepping control, genetic control, neural network control, and fuzzy control. Different control algorithms have their advantages and disadvantages. For the adaptive control [10–12], the controller is able to learn itself and adapt to variations of the dynamics and hydrodynamic coefficients of the system. But the selection of the key parameters is complex. For the suboptimal control, [13] puts forward an approach which is decoupling the model or dismissing the nonaffine terms when designing the suboptimal control schemes. However, the coupling terms must be considered in the control system, or the accuracy of the model will be decreased. For the backstepping control [14], backstepping control techniques were used to force the errors of the system to an arbitrarily small neighborhood of zero. Nevertheless, the system has a longer settling time. For the genetic control [15], the genetic algorithm has to encode and decode a mass of data, which it will spend a long time to calculate, and the quick response cannot be guaranteed. For the neural network control [16], the algorithms cannot keep the stability at a better level because the optimal weight is of strong dependence in the input. For the fuzzy control, a fuzzy sliding mode controller proposed in [17] is designed for path tracking in the horizontal plane, but the convergence time is too long. Also, many scholars, such as G. W. Weber, E. Kropat, and T. Paksoy et al., carried out immense amounts of concrete researches in different fields which include environment prediction, free market trading, and resource allocation [18–21]. In their study, the characteristics of the research object are in

common which are uncertain parameters, strong hysteresis, and high dependence to initial state. On account of the similar features which the AUV introduced in this paper has, the fuzzy control methods can be learned from.

As sliding mode control is based on the sliding mode surfaces, the stability and rapidity are evident if the Lyapunov equation is right established. Hence, sliding mode control becomes popular. Furthermore, sliding mode control is with strong robustness against model uncertainties and external environmental disturbances [22–24]. Therefore, the sliding mode control does not need strict requirements on the accuracy of the model, and, at the same time, it can ensure the stability, the accuracy, and the rapidity as well as parameters' easy tuning. However, the model adopted in this paper is of big difference from most AUVs on account of its large inertia and large scale.

In this paper, based on the advantages of each control algorithm introduced above and then doing further optimizing, a novel fuzzy iterative sliding mode control scheme is presented which introduces a hyperbolic tangent function in multiple sliding mode surfaces and control laws and uses fuzzy logic to tune the parameters automatically. Due to the boundedness of the hyperbolic tangent function, the controller will also be bounded. It is concluded that the stability, the accuracy, and the rapidity of the system can be in favorable control. In this way, FISMC is more suitable for engineering applications.

The rest of this paper is organized as follows: Section 2 presents the kinematic and kinetic model of the AUV. The next section describes the design of the proposed controller based on line-of-sight guidance law, iterative sliding mode surfaces, and fuzzy logic. A set of comparative simulations are conducted in Section 4 to test the performance among the newly designed controller and other controllers. In the final section, conclusions and future work are discussed.

2. Problem Statement

2.1. Modeling of the AUV. The purpose of modeling for the AUV is to establish kinematic and kinetic equations. The kinematic model deals with geometrical aspects of motion, while the kinetic model focuses on the active and passive forces and moments about the vehicle [25]. In this paper, 3D path following is considered; hence, the AUV's motion in 3D space must be taken into consideration, which involves displacements and rotations in the 3D space, that is, the surge, sway, heave, roll, pitch, and yaw motion [26].

As shown in Figure 1, the earth-fixed and body-fixed reference frame are represented with {E} and {B}. The origin of the frame {B} is fixed at the AUV's center of gravity with the x-axis forward, the y-axis right, and the z-axis down. Also, the motion in the roll direction around the x-axis is positive counterclockwise, the pitch motion around the y-axis is positive bow-up, and the yaw motion around the z-axis is positive turning left. The linear velocities u, v, w are along with the x-, y-, z-axes, respectively, and the angular velocities p, q, r are rotated around the x-, y-, z-axes, respectively.

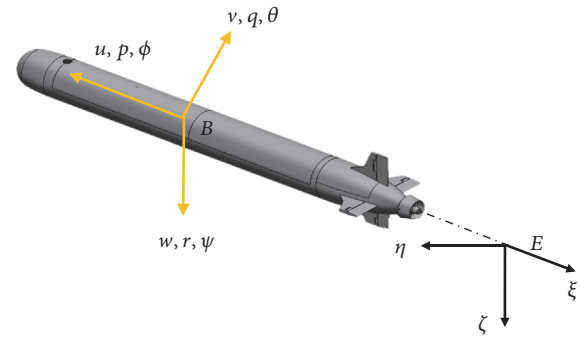

Figure 1: Definition of coordinate frames.

The AUV has neutrally buoyant and hydrodynamic restoring forces which are large enough to neglect the roll motion in 3D space; the model of the AUV can be described as following the kinetic and kinematic model.

$$
\begin{aligned}
\dot{u} &= X_{uu}u^2 + X_{vv}v^2 + X_{ww}w^2 + X_{vr}vr + X_{wq}wq \\
&\quad + X_{qq}q^2 + X_{rr}r^2 + X_{\delta_s\delta_s}u^2{\delta_s}^2 + X_T + F_{X_{dis}} \\
\dot{v} &= Y_v uv + Y_r ur + Y_{vw}vw + Y_{vq}vq + Y_{v|v|}v\left|v_0\right| \\
&\quad + Y_{v|r|}\frac{v}{|v|}\left|v_0\right|\left|r\right| + Y_{|v|r}\left|v_0\right|r + Y_{wr}wr + Y_{qr}qr \\
&\quad + Y_{r|r|}r\left|r\right| + Y_{\delta_r}u^2\delta_r + F_{Y_{dis}} \\
\dot{w} &= Z_w uw + Z_{|w|}uw + Z_q uq + Z_\theta\theta + Z_{vv}v^2 + Z_{vr}vr \\
&\quad + Z_{ww}\left|ww_0\right| + Z_{w|w|}w\left|w_0\right| + Z_{w|q|}\frac{w}{|w|}\left|w_0\right|\left|q\right| \\
&\quad + Z_{|w|q}\left|w_0\right|q + Z_{|q|q}q\left|q\right| + Z_{rr}r^2 + Z_{\delta_s}u^2\delta_s \\
&\quad + Z_{|q|\delta_s}u\left|q\right|\delta_s + F_{Z_{dis}} \\
\dot{p} &= K_v uv + K_r ur + K_{vw}vw + K_{v|v|}v\left|v_0\right| + K_{vq}vq \\
&\quad + K_{|v|r}\left|v_0\right|r + K_{v|r|}\frac{v}{|v|}\left|v_0\right|\left|r\right| + K_{wr}wr \\
&\quad + K_{qr}qr + K_{r|r|}r\left|r\right| + K_{\delta_r}u^2\delta_r + K_{X_{dis}} \\
\dot{q} &= M_w uw + M_{|w|}u\left|w\right| + M_q uq + M_\theta\theta + M_{vv}v^2 \\
&\quad + M_{rr}vr + M_{ww}\left|ww_0\right| + M_{w|w|}w\left|w_0\right| \\
&\quad + M_{w|q|}\frac{w}{|w|}\left|w_0q\right| + M_{|w|q}\left|w_0\right|q + M_{q|q|}q\left|q\right| \\
&\quad + M_{rr}r^2 + M_{\delta_s}u^2\delta_s + M_{|q|\delta_s}u\left|q\right|\delta_s + M_{Y_{dis}} \\
\dot{r} &= N_v uv + N_r ur + N_{vw}vw + N_{v|v|}v\left|w_0\right| + N_{vq}vq \\
&\quad + N_{|v|r}\left|v_0\right|r + N_{r|r|}\frac{v}{|v|}\left|v_0\right|\left|r\right| + N_{wr}wr \\
&\quad + N_{qr}qr + N_{r|r|}r\left|r\right| + N_{\delta_r}u^2\delta_r + N_{Z_{dis}}
\end{aligned}
\tag{1}
$$

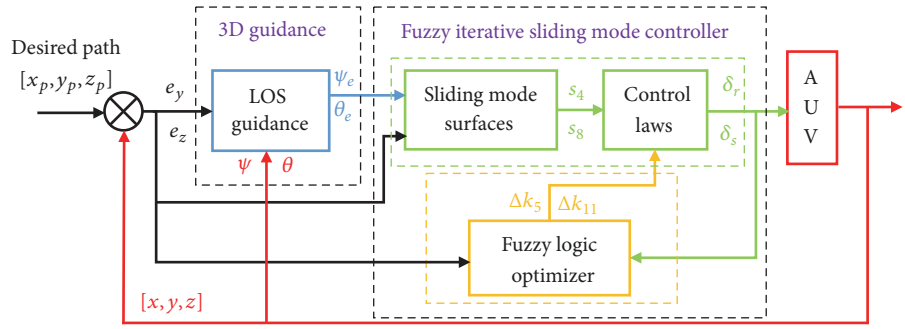

Figure 2: Control framework of 3D path following.

$$\begin{aligned}\dot{\xi} &= u\cos\psi\cos\theta - v\sin\psi + w\sin\theta\cos\psi\\ \dot{\eta} &= u\sin\psi\cos\theta + v\cos\psi + w\sin\theta\sin\psi\\ \dot{\zeta} &= -u\sin\theta + w\cos\theta.\end{aligned} \tag{2}$$

The detailed descriptions of the model and parameters in formulas (1) and (2) can be found in [27].

2.2. Problem Formulation. The AUV in this paper is characteristic with a large scale, large inertia, and high speed. With these special features, controller designing of this AUV is much more difficult and of higher requirements in terms of stability, accuracy, and rapidity.

For example, in order to drive the vehicle and converge to a predefined path, there are so many parameters by using the PID controller, such as input variable, error of present and desired heading angle, and output variable and control-rudder angle. In addition, the parameters in the PID controller are sensitive to the AUV's initial position, initial attitude, environmental disturbances, and so on. The drawback of the PID controller applied for this AUV will be illustrated in detail by simulation results in Section 4.

The 3D path following problem deals with the design of control law which could control this kind of special AUV with a large scale, large inertia, and high speed to reach a desired path stably, accurately, and rapidly. The control objectives are as follows:

$$\begin{aligned}\lim_{t\to\infty}\varepsilon(t) &= 0\\ \lim_{t\to\infty}U(t) &= U_p.\end{aligned} \tag{3}$$

Deriving a control law so that the position error ε between the AUV's present position (x, y, z) and desired position (x_p, y_p, z_p) converges to zero asymptotically, the current resultant velocity U tends to the desired resultant velocity U_p.

3. 3D Path Following Controller Design

In this section, the two-layered control framework is established for 3D path following of the AUV. As presented in Figure 2, the control framework includes a 3D line-of-sight (LOS) guidance layer and a fuzzy iterative sliding mode control layer.

The input of the control system is the desired path (x_p, y_p, z_p) given in advance, while the present position (x, y, z) and the present attitude angle (ψ, θ) of the AUV are outputs. The respective heading angle and pitch angle are acquired from 3D guidance laws. Then, the sliding mode surfaces and control law are introduced to regulate the outputs of the actuators. By using the fuzzy logic optimizer with inputs which include errors of the path (y_e, z_e) and rudder angles (δ_r, δ_s), outputs Δk_5 and Δk_{11} are added to automatically tune FISMC parameters. Hence, the performance of the 3D path following controller is obviously improved.

3.1. LOS Guidance Law for Path Following. In this subsection, the LOS guidance law for path following is presented. The 3D motion of the AUV can be divided into motions in two different planes which are the horizontal plane and vertical plane, respectively.

Control objectives of path following need to meet the following two requirements [28]:

(1) Decreasing the offset distance between the AUV's position and the desired position to zero

(2) Aligning the direction between the AUV's velocity vector and the desired path's tangential vector

As shown in Figure 3, the AUV follows the desired curvilinear path S which is marked in the green color. The red dot "O" is the present position of the AUV in the earth-fixed frame {E} while the pink dot "F" represents the current target point in reference path S, and the blue dot "R" is the next target point which is along with the desired path's tangential vector. Introducing the Serret-Frenet coordinate frame {P} taking the current target point "F" at the origin, and considering the rotation from path frame {P} to fixed frame {E}, the path following error vector $[x_e, y_e, z_e]^T$ can be written as

$$\begin{aligned}x_e &= \cos(\psi_p)\cos(\theta_p)(x - x_p)\\ &\quad + \sin(\psi_p)\cos(\theta_p)(y - y_p)\\ &\quad - \sin(\theta_p)(z - z_p)\\ y_e &= -\sin(\psi_p)(x - x_p) + \cos(\psi_p)(y - y_p)\end{aligned}$$

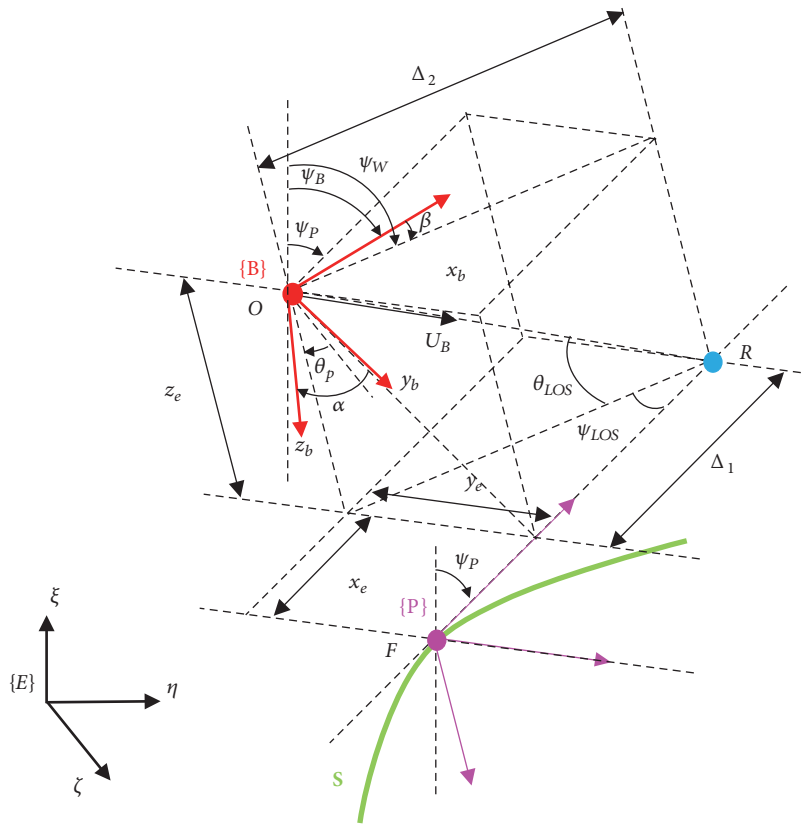

Figure 3: Path following in 3D space.

$$\begin{aligned} z_e &= \cos\left(\psi_p\right)\sin\left(\theta_p\right)\left(x - x_p\right) \\ &\quad + \sin\left(\psi_p\right)\sin\left(\theta_p\right)\left(y - y_p\right) \\ &\quad + \cos\left(\theta_p\right)\left(z - z_p\right). \end{aligned} \tag{4}$$

The line-of-sight (LOS) guidance angle in the horizontal plane named azimuth angle ψ_{LOS} is designed as

$$\psi_{LOS} = \arctan\left(\frac{y_p - y_q}{\Delta_1}\right), \tag{5}$$

where $(\Delta_1, 0)$ is the coordinate of the next followed target point in moving frame {P}, Δ_1 is a positive constant, and (x_q, y_q) is the coordinate of the next followed target point in the earth-fixed frame {E}, that is, absolute position coordinates.

Analyzing Figure 3, the value of $(y_p - y_q)$ in the earth-fixed frame {E} equals y_e in frame {P}, so ψ_{LOS} is rewritten as

$$\psi_{LOS} = \arctan\left(-k_\psi \cdot y_e\right) > 0, \tag{6}$$

where the control gain $k_\psi = -1/\Delta_1 > 0$.

As $\psi_{LOS} = \psi_W - \psi_P$ and $\psi_d = \psi_B = \psi_W - \beta$, the desired yaw angle under the LOS guidance of path following can be defined as

$$\psi_d = \arctan\left(-k_\psi \cdot y_e\right) + \psi_P - \beta, \tag{7}$$

where $\beta = \arctan(v/u)$ is the side-slip angle of the AUV.

Similarly, the elevation angle θ_{LOS} and pitch angle θ_d in the vertical plane are depicted as

$$\begin{aligned} \theta_{LOS} &= \arctan\left(k_\theta \cdot z_e\right) \\ \theta_d &= \arctan\left(k_\theta \cdot z_e\right) - \theta_p + \alpha, \end{aligned} \tag{8}$$

where $\alpha = \arctan(w/u)$ is the angle of attack and the control gain $k_\theta > 0$. Here, the signs of (6), (7), and (8) should be noted.

3.2. Fuzzy Iterative Sliding Mode Controller Design. As previously mentioned, the PID control scheme lacks robustness and could not keep the accuracy while guaranteeing the rapidity. To solve this problem, a fuzzy iterative sliding mode controller based on the LOS guidance law is designed in this subsection. More than one of the sliding mode nonlinear surfaces settle the contradiction between static performance and dynamic performance of the control system which mainly refer to errors of the steady state and time of approaching the steady state, respectively. In this way the controller can ensure the robustness and the adaptability, despite of system uncertainties and environmental unknown disturbances. Next, application of fuzzy logic heuristic knowledge further enhances the self-adaptability which makes it more convenient to tune the parameters of the controller automatically.

Theorem 1. *Consider the nonlinear scalar system with zero order defined as* $s_n = f(x, u, t)$, *where* $x, u, s \in \mathbb{R}$ *are system*

state variable, system input, and system output, respectively. If the following conditions are established:

(I) *The equation of state is* $\dot{x} = g(u)$*, where* $g(u)$ *is a continuous and bounded function*

(II) $f(x,u,t)$ *is a continuous, bounded, and nonlinear function, namely,* $|\partial f/\partial x| < \sigma$*, and* σ *is a bounded value*

(III) *Sign for the gain of output* s_n *to input* u *is known; here assume that* $\partial f/\partial u > 0$

the incremental feedback control law is chosen as

$$\dot{u} = -k_t s_n - \varepsilon \tanh(s_n), \tag{9}$$

where $k_t, \varepsilon \in \mathbb{R}^+$.

Based on the proposed conditions and control law above, the system s_n *can realize asymptotic stability.*

Proof. Choose the following Lyapunov function candidate:

$$V = \frac{1}{2} {s_n}^2. \tag{10}$$

Taking the derivative of formula (10), one can get

$$\dot{s}_n = \frac{\partial f}{\partial x}\dot{x} + \frac{\partial f}{\partial u}\dot{u}. \tag{11}$$

By using formulas (9) and (11), the time derivative of the proposed Lyapunov function is such that

$$\begin{aligned} \dot{V} &= s_n \dot{s}_n = s_n \left(\frac{\partial f}{\partial x}\dot{x} + \frac{\partial f}{\partial u}\dot{u} \right) \\ &= \frac{\partial f}{\partial x}\dot{x}y + \frac{\partial f}{\partial u}\left[-k_t s_n - \varepsilon \tanh(s_n) \right] y \\ &\le -\left\{ \frac{\partial f}{\partial u}\left[-k_t |s_n| + \varepsilon \left| \tanh(s_n) \right| \right] - \sigma g(u) \right\} |y|. \end{aligned} \tag{12}$$

As $\partial f/\partial u > 0$ and σ is bounded, it is clear that

$$\frac{\partial f}{\partial u}\left[-k_t |s_n| + \varepsilon \left| \tanh(s_n) \right| \right] - \frac{\partial f}{\partial u} g(u) > 0 \tag{13}$$

with existing $k_t, \varepsilon \in \mathbb{R}^+$, that is, $V < 0$.

Therefore, it can be concluded that the system s_n can realize asymptotic stability according to the Lyapunov stability criterion.

According to the features of the AUV in this paper, the revolving speed of the propeller is fixed. Aiming at the actuators of the AUV, yaw rudder, and horizontal rudder, the controllers used for the horizontal plane and vertical plane are designed, respectively. □

Theorem 2. *In the horizontal plane, iterative sliding mode control surfaces are given as follows:*

$$\begin{aligned} s_1(y_e) &= k_1 \tanh(k_0 y_e) + \dot{y}_e \\ s_2(s_1, \psi_e) &= k_2 \int \tanh(s_1)\, d_t + \psi_e \\ s_3(s_2) &= k_3 \tanh(s_2) + \dot{s}_2 \\ s_4(s_3) &= k_4 \tanh(s_3) + \dot{s}_3 \end{aligned} \tag{14}$$

and the control law combined with sliding mode surfaces is defined as

$$\dot{\delta}_r = -k_5 s_4 - \varepsilon_1 \tanh(s_4), \tag{15}$$

where $k_0, k_1, k_2, k_3, k_4, k_5, \varepsilon_1 \in \mathbb{R}^+$ *and* $k_3 \le k_4$.

When applying to the controller with defined surfaces (14) and control law (15), it can guarantee the errors of path following in the horizontal plane for the AUV asymptotic convergence to zero.

Proof. Expanding formula (14), one can obtain

$$\begin{aligned} s_4 &= k_4 \tanh(s_3) + \left[k_3 \tanh(s_2) + \dot{s}_2 \right]' \\ &= k_4 \tanh(s_3) + \left\{ k_3 \left[1 - \tanh^2(s_2) \right] \dot{s}_2 + \ddot{s}_2 \right\} \\ &= k_4 \tanh(s_3) + \frac{k_3 \left[k_2 \int \tanh(s_1)\, d_t + \psi_e \right]'}{\cosh^2(s_2)} + {\psi_e}'' \\ &\quad + k_2 \left[1 - \tanh^2(s_1) \right] \dot{s}_1 \\ &= k_4 \tanh(s_3) + \frac{k_3 \left[k_2 \int \tanh(s_1)\, d_t + \psi_e \right]'}{\cosh^2(s_2)} + \dot{r} \\ &\quad + \frac{k_2 \left[k_1 \tanh(k_0 y_e) + \dot{y}_e \right]'}{\cosh^2(s_1)} \\ &= k_4 \tanh(s_3) + \frac{k_3 \left[k_2 \int \tanh(s_1)\, d_t + \psi_e \right]'}{\cosh^2(s_2)} + \dot{r} \\ &\quad + \frac{k_2 \left\{ k_1 k_0 \dot{y}_e / \cosh^2(k_0 y_e) + \ddot{y}_e \right\}}{\cosh^2(s_1)}. \end{aligned} \tag{16}$$

Analyzing formula (14), information can be gotten as follows.

Due to the surface s_4 with second-order derivative terms in ψ_e, namely, control-rudder δ_r, one can obtain

$$\begin{aligned} \frac{\partial h(s_4)}{\partial \delta_r} &\not\equiv 0, \\ \frac{\partial h(s_3)}{\partial \delta_r} &= 0, \\ \frac{\partial h(s_2)}{\partial \delta_r} &= 0, \\ \frac{\partial h(s_1)}{\partial \delta_r} &= 0, \end{aligned} \tag{17}$$

where $h(s_n)$ $(n = 1, 2, 3, 4)$ are the functions of s_n.

Substituting formula (17) in (16), one can get

$$\frac{\partial s_4}{\partial \delta_r} = \frac{\partial}{\partial \delta_r}\left(\dot{r} + \frac{k_2 \ddot{y}_e}{\cosh^2(s_1)} \right). \tag{18}$$

Next, analyzing formulas (1) and (2), information can be gotten as follows.

On one hand, the signs of velocities u, v, r keep the same as yaw rudder δ_r. On the other hand, the values of $w, q, \dot{v}$ are absolutely small due to steering yaw rudder; one can get

$$\frac{\partial s_4}{\partial \delta_r} = \frac{\partial}{(\partial \delta_r)\left(M_R/\left(J_z + \triangle J_z\right) + k_2 \ddot{y}_e/\cosh^2(s_1)\right)}$$
$$\frac{M_R}{J_z + \triangle J_z} > 0, \tag{19}$$

where M_R refers to the moment of force caused by steering yaw rudder, J_z refers to the moment of inertia for the AUV body, and $\triangle J_z$ refers to the additional moment of inertia for the hydrodynamic force.

Go on analyzing formulas (1) and (2); information can be obtained as follows.

$\ddot{y}_e$ is related to the acceleration caused by forces of the propeller and yaw rudder. And the forces split into two components which are a force F_{X_R} along with the x-axis and a force F_{Y_R} along with the y-axis. One can get

$$\frac{\partial s_4}{\partial \delta_r} = \frac{\partial}{\partial \delta_r}\left(\frac{M_R}{J_z + \triangle J_z} + \frac{k_2\left[F_{X_R}/\left(m + m_x\right) + F_{Y_R}/\left(m + m_y\right)\right]}{\cosh^2(s_1)}\right), \tag{20}$$

where m_x, m_y refer to the additional mass for the hydrodynamic force.

Considering the case of steering yaw rudder in the horizontal plane, the values of F_{X_R} and F_{Y_R} are far less than M_R, due to the boundedness of the hyperbolic trigonometric function; it can be concluded that

$$\frac{\partial s_4}{\partial \delta_r} > 0 \tag{21}$$

with existing k_2.

Based on formula (21), surface s_4 asymptotically converges to zero with defined control law (15).

As $s_4 = 0$, according to the mathematical relationship among surfaces s_4, s_3, s_2, it is clear that

$$s_3 = 0,$$
$$s_2 = 0. \tag{22}$$

When $s_2 \longrightarrow 0$, it yields that

$$\psi_e = -k_2 \int \tanh(s_1)\, d_t$$
$$\dot{\psi}_e = -k_2 \tanh(s_1). \tag{23}$$

As the values of φ, θ, w are absolutely small while steering yaw rudder, and substituting for $\dot{y}_e$ into formula (14) from formula (2), one can get

$$s_1 = k_1 \tanh(k_0 y_e) + u \sin(\psi_e) + v \cos(\psi_e). \tag{24}$$

Obviously, s_1 is a continuous, bounded, and nonlinear function of ψ_e which can be deemed to be the control input as described in **Theorem 1**; one can obtain

$$\frac{\partial s_1}{\partial \psi_e} = u \cos(\psi_e) - v \sin(\psi_e). \tag{25}$$

Because of the characteristic of the AUV which voyages forward at a fixed speed, that is to say, $u \in \mathbb{R}^+$ is a constant, and because the value of forward velocity u is more than lateral velocity v, it is easy to conclude that

$$\frac{\partial s_1}{\partial \psi_e} = u \cos(\psi_e) - v \sin(\psi_e) > 0 \tag{26}$$

when $|\psi_e| < \pi/2$.

Based on Theorem 1, the surface s_1 can asymptotically converge to zero under the control law chosen as formula (15); it yields that

$$\dot{y}_e \longrightarrow -k_1 \tanh(k_0 y_e). \tag{27}$$

Due to the uniform monotonicity of y_e and $\tanh(k_0 y_e)$ while $\dot{y}_e$ has the opposite monotonicity of $\tanh(k_0 y_e)$, it is evident that

$$y_e \longrightarrow 0. \tag{28}$$

Therefore, the errors of path following for the AUV asymptotically convergence to zero. □

Theorem 3. *In the vertical plane, iterative sliding mode control surfaces and control law are given as follows:*

$$s_5(z_e) = k_7 \tanh(k_6 z_e) + \dot{z}_e,$$
$$s_6(s_5, \theta_e) = k_8 \int \tanh(s_5)\, d_t + \theta_e$$
$$s_7(s_6) = k_9 \tanh(s_6) + \dot{s}_6$$
$$s_8(s_7) = k_{10} \tanh(s_7) + \dot{s}_7$$
$$\dot{\delta}_s = -k_{11} s_8 - \varepsilon_2 \tanh(s_8) \tag{29}$$

where $k_6, k_7, k_8, k_9, k_{10}, k_{11}, \varepsilon_2 \in \mathbb{R}^+$ *and* $k_9 \le k_{10}$.

When applying to the controller with defined surfaces and control law (29), it can guarantee the errors of path following in the vertical plane for the AUV asymptotic convergence to zero.

Proof. The proving process can be in a similar method and it is omitted. □

Based on ISMC, the FISMC focuses on the self-adaptability of control parameters which guarantee the AUV with environmental disturbance rejection and inhibition of chattering for the rudder.

Analyzing the control laws $\dot{\delta}_r, \dot{\delta}_s$ in formulas (15) and (29), it is clear that parameters k_5, k_{11} determine the efficiency and robustness of the control system. Consequently, fuzzy logics are introduced to tune k_5, k_{11} automatically.

Table 1: Fuzzy logic rules for Δk_5.

Δk_5		δ_r						
		NB	NM	NS	Z	PS	PM	PB
y_e	NB	NB	NB	NB	NB	NB	NB	NB
	NM	NM	NM	NM	NM	NM	NM	NM
	NS	PS	PS	PS	PB	PS	PS	PS
	Z	PS	PM	PS	Z	PS	PM	PS
	PS	PS	PM	PS	PB	PS	PM	PS
	PM	NM	NM	NM	NM	NM	NM	NM
	PB	NB	NB	NB	NB	NB	NB	NB

Table 2: Fuzzy logic rules for Δk_{11}.

Δk_{11}		δ_s						
		NB	NM	NS	Z	PS	PM	PB
z_e	NB	NB	NB	NB	NB	NB	NB	NB
	NM	NM	NM	NM	NM	NM	NM	NM
	NS	PS	PS	PS	PB	PS	PS	PS
	Z	PS	PM	PS	Z	PS	PM	PS
	PS	PS	PM	PS	PB	PS	PM	PS
	PM	NM	NM	NM	NM	NM	NM	NM
	PB	NB	NB	NB	NB	NB	NB	NB

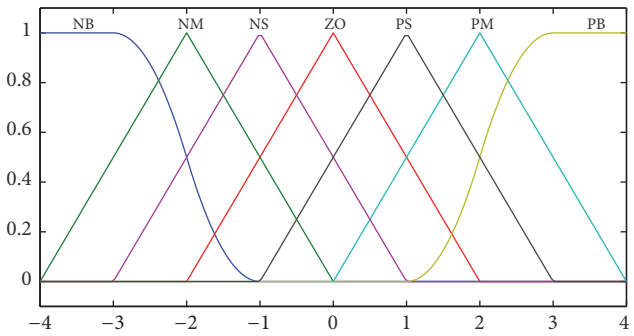

Figure 4: Membership function.

The fuzzy logic rules for the parameters Δk_5, Δk_{11} are shown in Tables 1 and 2. In Table 1, the first column represents fuzzy subsets for the following errors of the path y_e while the first row is fuzzy subsets for the control-rudder δ_r. Also, other cells represent the evaluating values of outputs. All of the inputs and outputs keep the IF-THEN rules. Table 2 is set the same as Table 1.

The fuzzy subsets are divided into traditional types which are NB, NM, NS, ZE, PS, PM, and PB, respectively, namely, negative big, negative medium, negative small, zero, positive small, positive medium, and positive big. The input scaling factors of $y_e, \delta_r, z_e, \delta_s$ are $g_{y_e}, g_{\delta_r}, g_{z_e}, g_{\delta_s}$, respectively, while the output scaling factors of $\Delta k_5, \Delta k_{11}$ are $g_{k_5}, g_{k_{11}}$. The fuzzification of $\Delta k_5, \Delta k_{11}$ is designed by the triangular membership function shown in Figure 4 while introducing centroid defuzzification.

Table 3: Key parameters of the AUV.

Parameter name	Parameter signal	Value
Mass	m	**2218.28 t**
Length	L	**80 m**
Breadth	B	6 m
Height	H	6 m
Displacement	∇	**1500 m^3**
Speed	u	**12 kn**

4. Numerical Simulation Research

Numerical simulation researches are performed to test the performance of the proposed control schemes in this paper through a special AUV whose key parameters are partly presented in Table 3. In the simulations, the AUV voyages with a fixed forward velocity, $u = 6$ m/s, due to a constant revolving speed in one direction of the propeller, and the desired route, $y_p = 500$, $z_p = 100$, which is 500 meters laterally and 100 meters vertically away from the initial route, $y_0 = 0, z_0 = 0$, is used to test the performance of the proposed controllers.

In the simulations, the delay time between the control signal and the actuators is considered according to the large-inertia feature of the AUV. The rudder control signals lag behind the yaw rudder and the horizontal rudder with 100 milliseconds, and the sample time in numerical simulation is 1 second.

It should be noted that the AUV mentioned in this paper has two water tanks, and the mass described in Table 3 includes the weight of the two water tanks and the weight of buoyancy force caused by the displacement. The existing advanced control algorithms are not applied to such large-scale underwater vehicles, and almost all of the submarine-like AUVs adopt the PID controller. In this way, different controllers commonly used in engineering are selected to verify the performance of the designed fuzzy iterative sliding mode control schemes. The control parameters are described as follows:

(i) PID parameters:

$$\begin{aligned} K_{p_h} &= 2 \times 10^{-5}, \\ K_{i_h} &= 5 \times 10^{-9}, \\ K_{d_h} &= 1.8, \\ K_{p_v} &= 3 \times 10^{-2}, \\ K_{i_v} &= 1.3 \times 10^{-8}, \\ K_{d_v} &= 0.5 \end{aligned} \tag{30}$$

(ii) ISMC parameters:

$$\begin{aligned} K_0 &= 0.01, \\ K_1 &= 1.5, \\ K_2 &= 0.05, \end{aligned}$$

$$
\begin{aligned}
K_3 &= 0.001,\\
K_4 &= 0.01,\\
K_5 &= 1,\\
\varepsilon_1 &= 1,\\
\Delta_1 &= \frac{1}{0.003}\\
K_6 &= 0.02,\\
K_7 &= 0.6,\\
K_8 &= 0.07,\\
K_9 &= 0.001,\\
K_{10} &= 0.01,\\
K_{11} &= 0.5,\\
\varepsilon_2 &= 1,\\
\Delta_2 &= \frac{1}{0.003}
\end{aligned}
\tag{31}
$$

(iii) FISMC parameters:

$$
\begin{aligned}
g_{y_e} &= \frac{4}{2},\\
g_{\delta_r} &= \frac{4}{2},\\
g_{z_e} &= \frac{4}{2},\\
g_{\delta_s} &= \frac{4}{2},\\
g_{k_5} &= \frac{4}{4},\\
g_{k_{11}} &= \frac{4}{4}
\end{aligned}
\tag{32}
$$

4.1. Simulation under Ideal Conditions. Figures 5–11 show the simulation results obtained under the conditions in which there are no environmental disturbances and the values of the AUV's initial position and attitude all equal zero.

In Figure 5, paths in 3D space along the desired path which is the green dot line and actual paths of the AUV using controllers marked in the black, red, and blue colors are shown. It is obvious that good path following of the AUV is achieved through each controller but with different performance.

More details can be noticed in Figure 6 which are, respectively, the projection of 3D paths in the horizontal plane and vertical plane. From this figure, it is illustrated that paths using the PID controller have big overshoots and oscillations. Nevertheless, paths of ISMC and FISMC converge to the desired path smoothly. Obviously, one should firstly try to avoid the overshoots and oscillations in controlling this kind of AUV with a large scale, large inertia, and high speed. At the same time, the time of approaching the steady state applying FISMC is shorter than the time with ISMC; this is more evidently shown in X-Z plane projection. Furthermore, errors of the steady state in FISMC are the smallest among the ISMC and PID controller. Note that it is difficult for the system to keep the shorter rising time as well as the smaller overshoots and the fewer oscillations simultaneously as a result of the parameters K_p, K_i with quite small orders of magnitude.

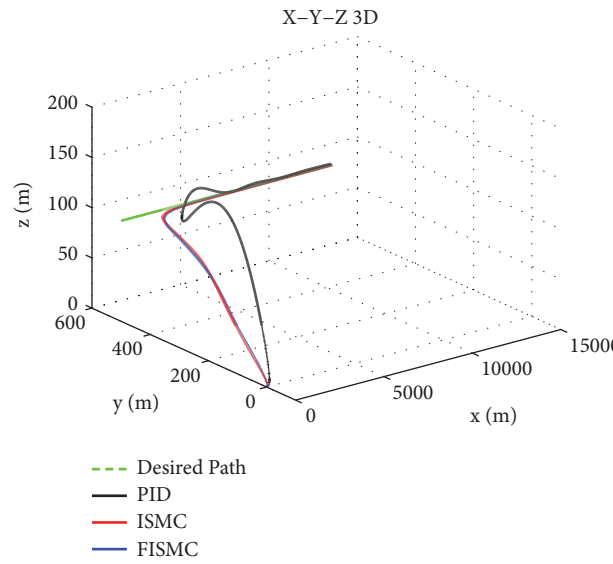

Figure 5: Paths in 3D space.

Focusing on the status of steering rudders from Figures 7 and 8, values of yaw rudder and horizontal rudder both converge to zero ultimately. But in controlling process, the chattering of the rudders when applying FISMC only happened one time, which is the lowest under the premise of keeping the stability, accuracy, and rapidity.

The changes of the desired angles ψ_d, θ_d depicted in Figure 9 map to the changes of paths in Figure 6.

Finally, regarding Figure 10, the convergence speed of surfaces s_1, s_2, s_3, s_4 in FISMC is much faster than ISMC's. This is also notable form surfaces s_5, s_6, s_7, s_8 shown in Figure 11. Meanwhile, the values of s_2, s_3, s_4 are decreasing progressively one by one as well as s_6, s_7, s_8 for the reason that surfaces are iterative. It further explains why fuzzy iterative sliding mode control can maintain better stability, accuracy, and especially rapidity than traditional sliding mode control with only one sliding surface.

4.2. Simulation under Environmental Disturbances. In this part, simulation is carried out under the environmental disturbance which is added from multiple directions in 3D space. Referring to formula (1), the decomposed force and moment can be described as

$$
\begin{aligned}
F_{X_{dis}} &= 0\\
F_{Y_{dis}} &= 0.11 \times 10^5 \sin\left[\frac{2\pi}{100\,(t-100)}\right]
\end{aligned}
$$

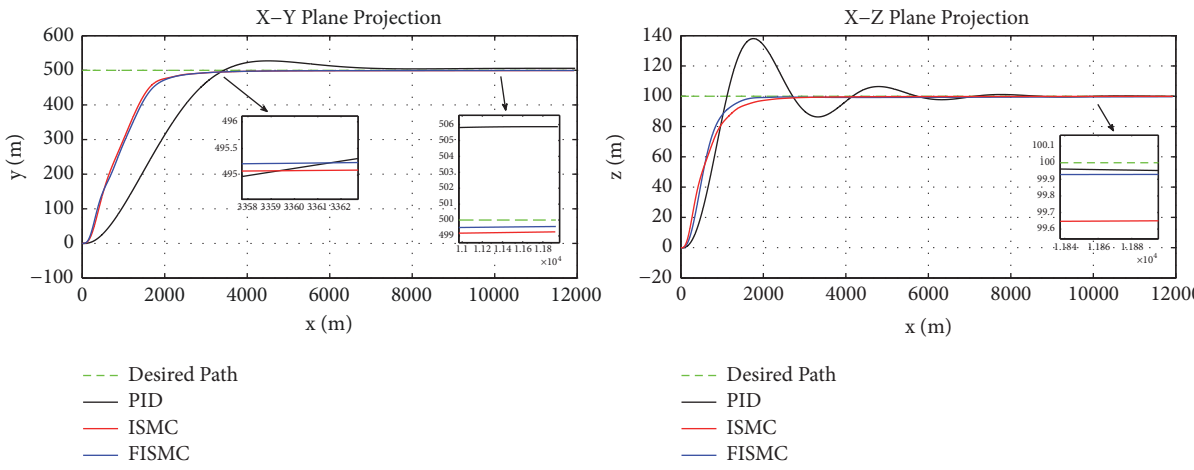

Figure 6: Paths in the horizontal plane and vertical plane.

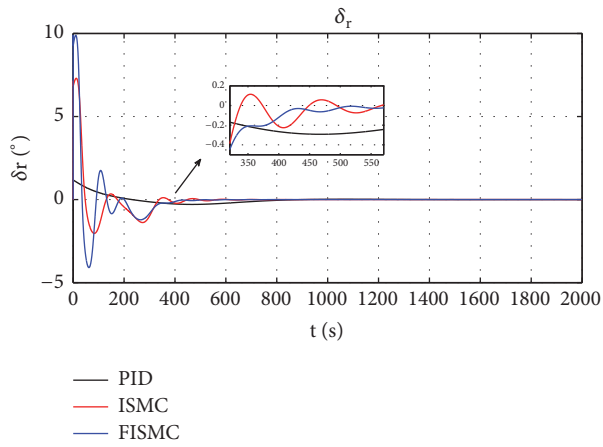

Figure 7: Yaw rudder.

$$F_{Z_{dis}} = 0.11 \times 10^5 \cos\left[\frac{2\pi}{100}(t - 100)\right]$$
$$K_{X_{dis}} = 0$$
$$M_{Y_{dis}} = F_{Y_{dis}} \times 40$$
$$N_{Z_{dis}} = F_{Z_{dis}} \times 40. \quad (33)$$

The time-varying disturbances which are an 11-ton force at maximum occur in the process of rising stage, 100 ~ 200 s, and steady state, 1200 ~ 1300 s. Compared with ideal conditions, simulation under environmental disturbances achieves better testing of three different controllers.

Glancing at Figure 12, paths differ from the paths shown in Figure 5, particularly in the stage of adding disturbances. To analyze the performance of the controllers, Figure 13 should be paid closer attention to.

Making a comparison with Figures 16 and 11, the approaching time is delayed for 20 s, and the overshoots of the PID controller increase. After all, there is a disturbance appended to the AUV body. Great differences can be noticed from the process of adding disturbances the second time. All three controllers are not able to avoid oscillations, but the performances are different from each other. In the PID controller, although its oscillation is approximately one time, it has the maximum deviation, 50 m in the lateral direction and 10 m in the vertical direction. Also, FISMC owns a lower number of oscillation with smaller deviation than ISMC. In the end, the minimal errors of the steady state appear in FISMC, not ISMC or PID.

4.3. Simulation under Different Initial Conditions. It can be basically estimated that FISMC provides the best performance when applying for path following of the AUV with large inertia. But in many cases, the AUV cannot start at zero initial conditions. For example, the initial heading angle of the AUV may not be zero absolutely. This comes to a question: If the special AUV is with the different initial heading angle, ψ_0, will the performances in one and the same controller be without distinction? Figures 14–16 explain the answer.

Figure 14 shows different actual paths of the AUV in the PID controller. It is obvious that different ψ_0 make a great difference in path following control. In spite of $\psi_0 = \pi/90$,

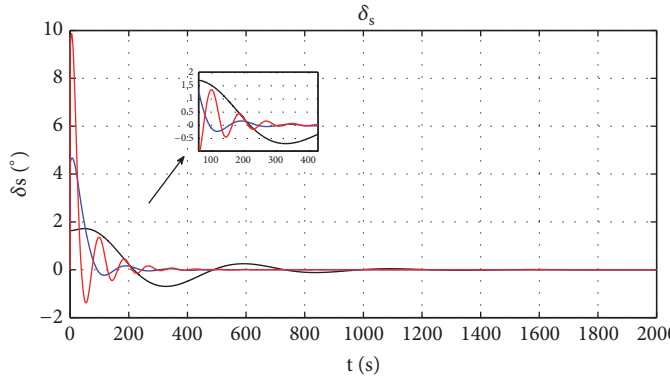

Figure 8: Horizontal rudder.

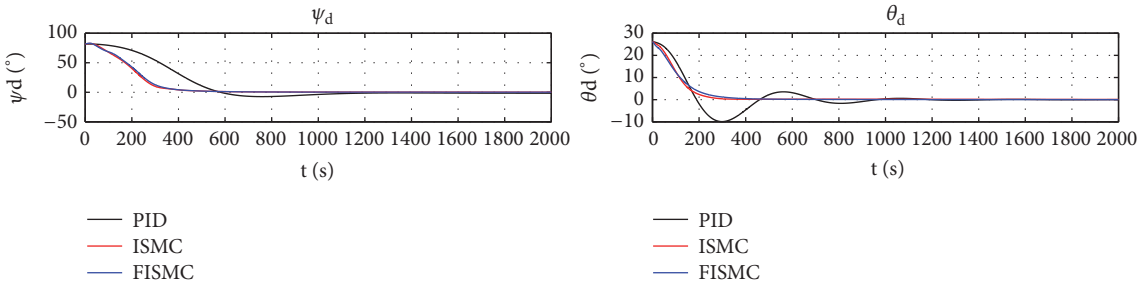

Figure 9: Heading angles and pith angles.

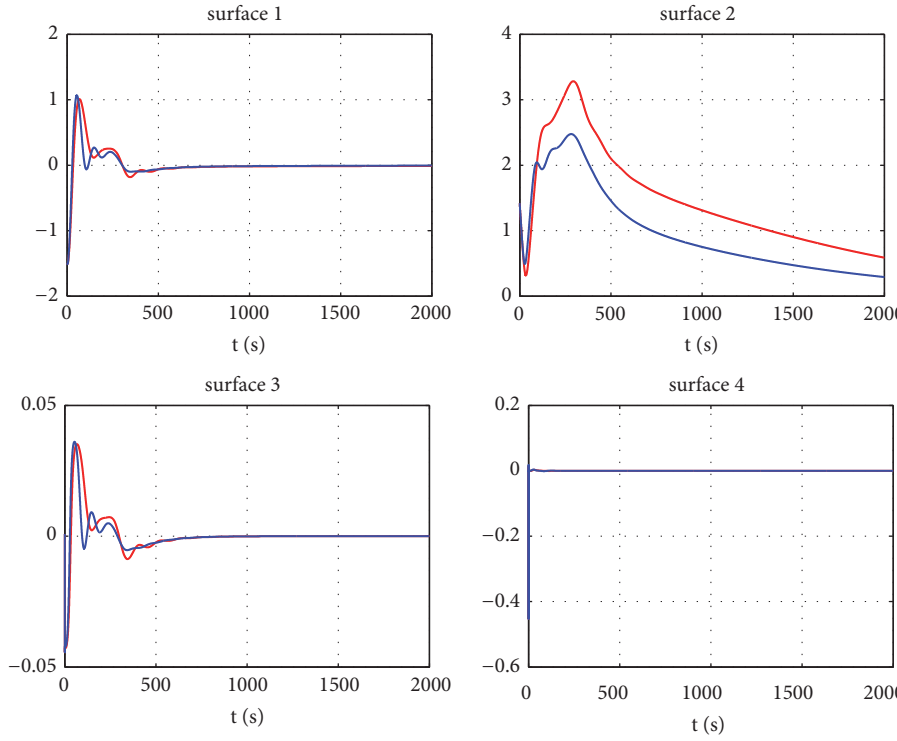

Figure 10: Sliding mode surfaces.

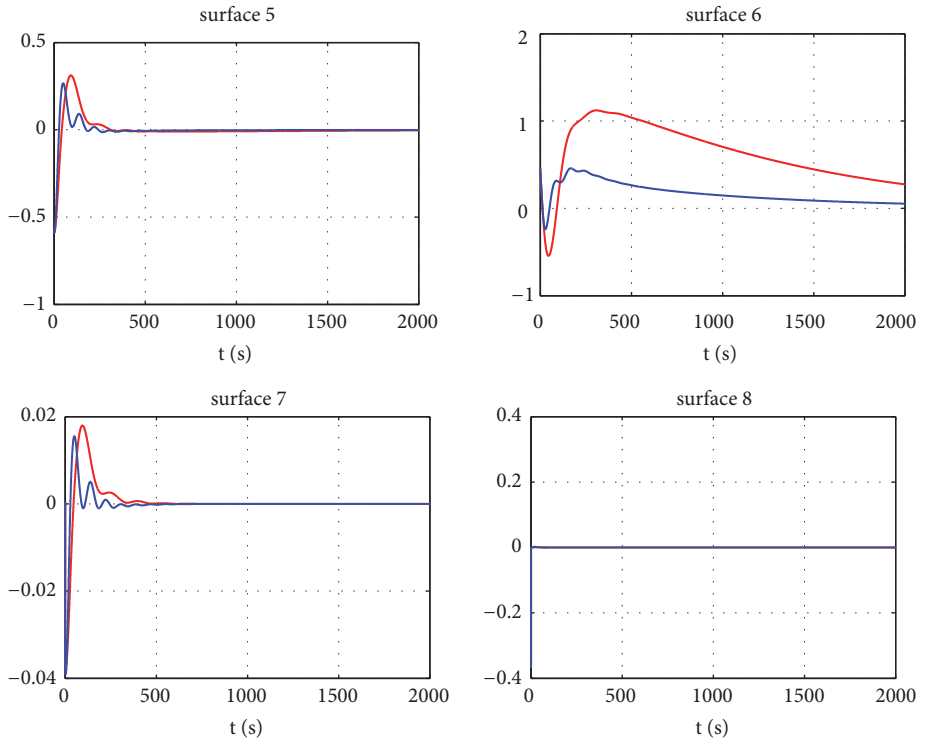

Figure 11: Sliding mode surfaces.

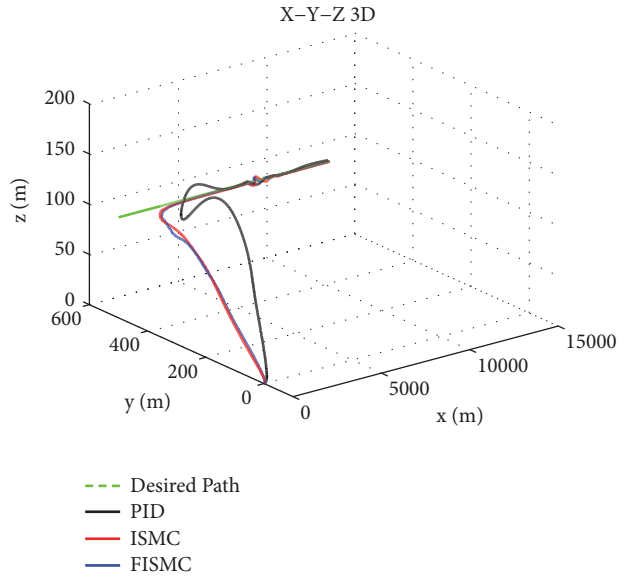

Figure 12: Paths in 3D space.

the error of the steady state in the horizontal plane is about 40 m marked in blue color; there is no need to consider other bigger ψ_0.

As Figure 15 explained, many simulation results prove the robustness of sliding mode control. With multiple initial heading angles $\psi_0 = 0, \pi/4, \pi/2, 3\pi/4, \pi, -\pi/4, -\pi/2, -3\pi/4$, actual paths in ISMC are different more or less. Even if $\psi_0 = \pi$ which means the direction of the AUV is completely opposite with $\psi_0 = 0$, the ISMC can adjust the AUV to follow the desired path. As is shown, overshoots exist in the actual paths when $|\psi_0|$ is big enough.

And making further improvement, the simulation used FISMC are carried out to be in contrast with ISMC. In Figure 16, the blue line is the path adopting FISMC and the red line is the path controlled by ISMC. It is clear that the overshoot disappears although there is a small amplitude

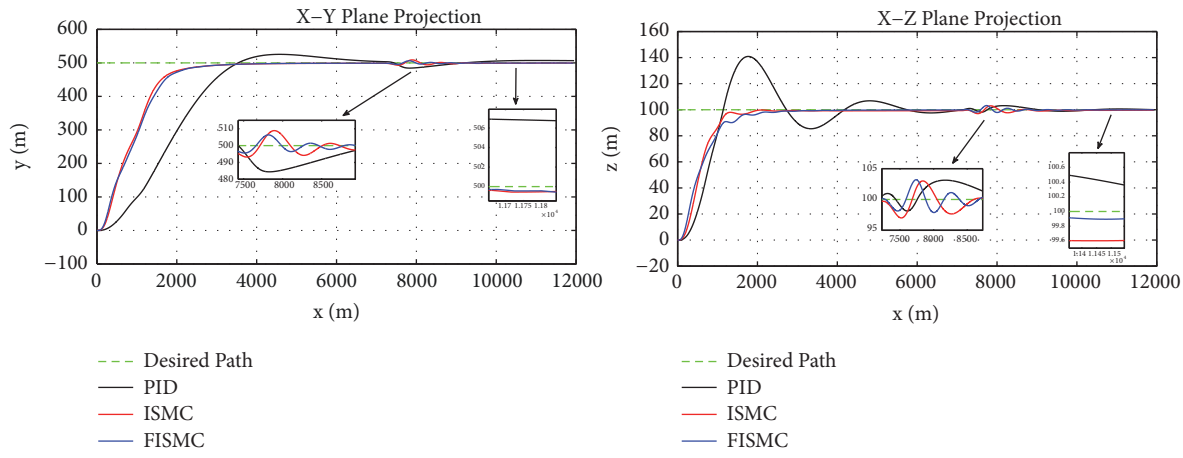

Figure 13: Paths in the horizontal plane and vertical plane.

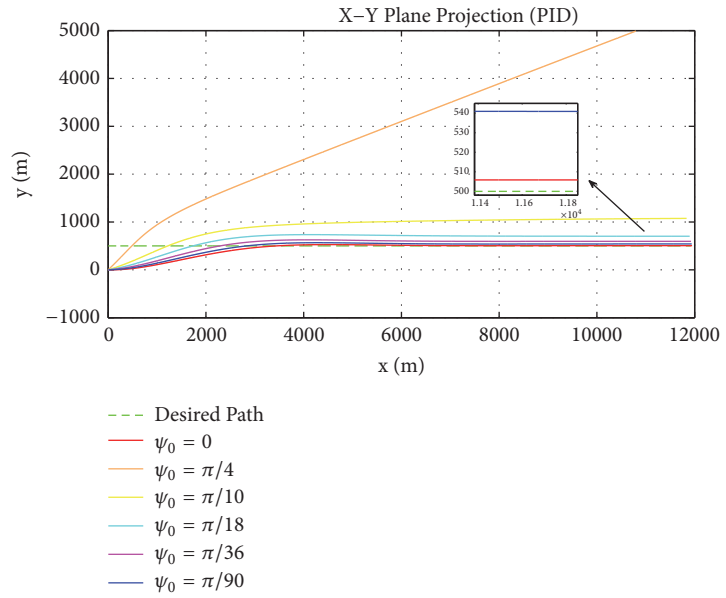

Figure 14: Paths in the horizontal plane with PID controller.

oscillation. The performance has been markedly improved on the foundation of ISMC.

In general, applying fuzzy iterative sliding mode control to the special AUV with a large scale, large inertia, and high speed, the performance can be guaranteed. Particularly when considering environmental disturbances and different initial state, the advantages of FISMC are evidently demonstrated.

5. Conclusion

This paper presented a novel fuzzy iterative sliding mode control scheme for the mentioned AUV. On the basis of previous research, the modeling of the AUV is introduced firstly, along with a problem formulation. Guidance laws for path following are then proposed applying the line-of-sight scheme. In this way, iterative sliding mode controller can be designed. Meanwhile, considering the self-adaptability of the control parameters, fuzzy logic is added on ISMC and then to form the FISMC. Finally, the robustness and self-adaptability of FISMC are verified through representative simulations. The AUV is able to complete path following while it is under environmental disturbances and various initial states.

Focusing on the results, the FISMC method can be applied to an underactuated vehicle with large-scale, large-inertia, and high-speed characters, in 2D and 3D path following, such as autopilot of oil tankers and cargo ships.

Data Availability

Partial data used to support the findings of this study are available from the corresponding author upon request.

Conflicts of Interest

The authors declare that they have no conflicts of interest.

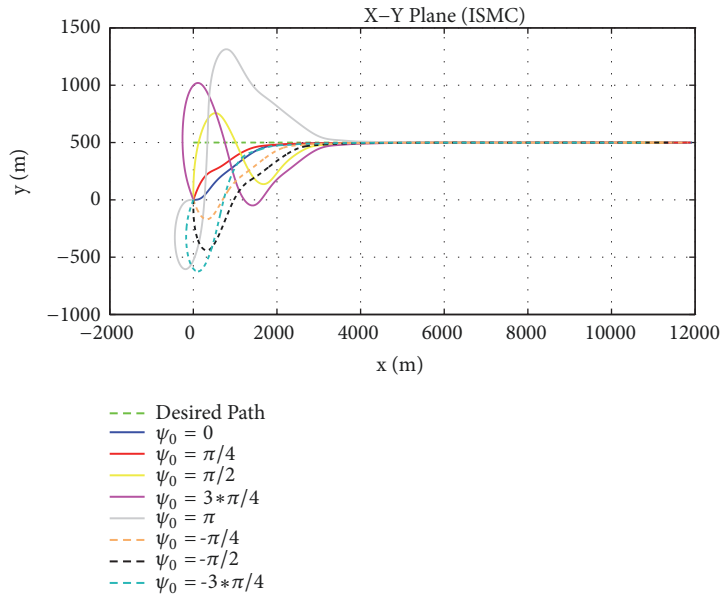

Figure 15: Paths in the horizontal plane with ISMC.

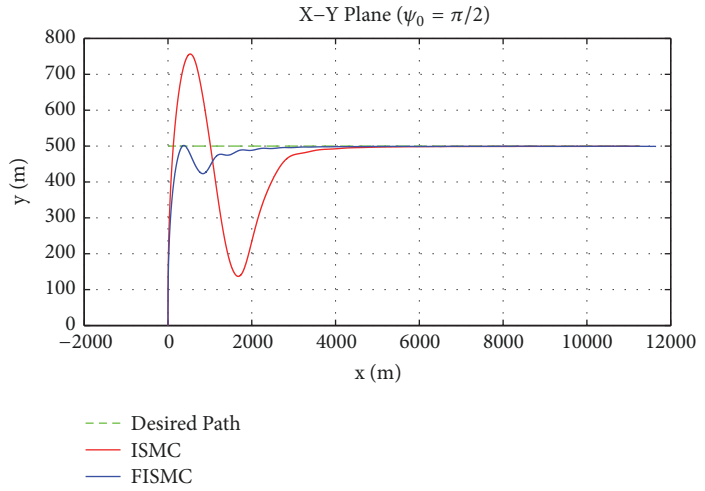

Figure 16: Paths in the horizontal plane controlled by ISMC and FISMC.

References

[1] X. Xiang, C. Yu, and Q. Zhang, "Robust fuzzy 3D path following for autonomous underwater vehicle subject to uncertainties," *Computers & Operations Research*, vol. 84, pp. 165–177, 2016.

[2] F. Zhang, G. Marani, R. N. Smith, and H. T. Choi, "Future trends in marine robotics," *IEEE Robotics and Automation Magazine*, vol. 22, no. 1, pp. 14–122, 2015.

[3] X. Xiang, C. Yu, J. Zheng, and G. Xu, "Motion forecast of intelligent underwater sampling apparatus — Part I: Design and algorithm," *Indian Journal of Geo-Marine Sciences*, vol. 44, no. 12, pp. 1962–1970, 2015.

[4] L. Lapierre and B. Jouvencel, "Robust nonlinear path-following control of an AUV," *IEEE Journal of Oceanic Engineering*, vol. 33, no. 2, pp. 89–102, 2008.

[5] R. Cui, S. S. Ge, B. Voon Ee How, and Y. Sang Choo, "Leader-follower formation control of underactuated autonomous underwater vehicles," *Ocean Engineering*, vol. 37, no. 17-18, pp. 1491–1502, 2010.

[6] X. B. Xiang, C. Y. Yu, L. Lapierre, J. L. Zhang, and Q. Zhang, "Survey on fuzzy-logic-based guidance and control of marine surface vehicles and underwater vehicles," *International Journal of Fuzzy Systems*, vol. 20, no. 2, pp. 572–586, 2018.

[7] X. B. Xiang, L. Lapierre, and B. Jouvencel, "Smooth transition of AUV motion control: from fully-actuated to under-actuated configuration," *Robotics and Autonomous Systems*, vol. 67, pp. 14–22, 2015.

[8] N. Wang and M. J. Er, "Direct adaptive fuzzy tracking control of marine vehicles with fully unknown parametric dynamics and uncertainties," *IEEE Transactions on Control Systems Technology*, vol. 99, pp. 1–8, 2016.

[9] N. Wang, S. Su, J. Yin, Z. Zheng, and M. J. Er, "Global Asymptotic Model-Free Trajectory-Independent Tracking Control of an Uncertain Marine Vehicle: An Adaptive Universe-Based

Fuzzy Control Approach," *IEEE Transactions on Fuzzy Systems*, vol. 26, no. 3, pp. 1613–1625, 2018.

[10] R. Cui, X. Zhang, and D. Cui, "Adaptive sliding-mode attitude control for autonomous underwater vehicles with input nonlinearities," *Ocean Engineering*, vol. 123, pp. 45–54, 2016.

[11] X. Qi, "Adaptive coordinated tracking control of multiple autonomous underwater vehicles," *Ocean Engineering*, vol. 91, pp. 84–90, 2014.

[12] B. K. Sahu and B. Subudhi, "Adaptive tracking control of an autonomous underwater vehicle," *International Journal of Automation and Computing*, vol. 11, no. 3, pp. 299–307, 2014.

[13] B. Geranmehr and S. R. Nekoo, "Nonlinear suboptimal control of fully coupled non-affine six-DOF autonomous underwater vehicle using the state-dependent Riccati equation," *Ocean Engineering*, vol. 96, pp. 248–257, 2015.

[14] F. Repoulias and E. Papadopoulos, "Planar trajectory planning and tracking control design for underactuated AUVs," *Ocean Engineering*, vol. 34, no. 11-12, pp. 1650–1667, 2007.

[15] E. Edison and T. Shima, "Integrated task assignment and path optimization for cooperating uninhabited aerial vehicles using genetic algorithms," *Computers & Operations Research*, vol. 38, no. 1, pp. 340–356, 2011.

[16] J. Lorentz and J. Yuh, "Survey and experimental study of neural network AUV control," in *Proceedings of the 1996 IEEE Symposium on Autonomous Underwater Vehicle Technology*, pp. 109–116, June 1996.

[17] N. Wang, J.-C. Sun, and M. J. Er, "Tracking-error-based universal adaptive fuzzy control for output tracking of nonlinear systems with completely unknown dynamics," *IEEE Transactions on Fuzzy Systems*, vol. 26, no. 2, pp. 869–883, 2018.

[18] E. Kropat and G. W. Weber, "Fuzzy target-environment networks and fuzzy-regression approaches," *Numerical Algebra, Control and Optimization*, vol. 8, no. 2, pp. 135–155, 2018.

[19] E. Kropat, A. Ozmen, G.-W. Weber et al., "Fuzzy prediction strategies for gene-environment networks-fuzzy regression analysis for two-modal regulatory systems," *RAIRO - Operations Research*, vol. 50, no. 2, pp. 413–435, 2016.

[20] S. K. Roy, A. Ebrahimnejad, J. L. Verdegay et al., "New approach for solving intuitionistic fuzzy multi-objective transportation problem," *Sādhanā*, vol. 43, no. 1, p. 3, 2018.

[21] T. Paksoy, T. Bektaş, and E. Özceylan, "Operational and environmental performance measures in a multi-product closed-loop supply chain," *Transportation Research Part E*, vol. 47, no. 4, pp. 532–546, 2011.

[22] Y. Feng, X. Yu, and Z. Man, "Non-singular terminal sliding mode control of rigid manipulators," *Automatica*, vol. 38, no. 12, pp. 2159–2167, 2002.

[23] M. B. R. Neila and D. Tarak, "Adaptive terminal sliding mode control for rigid robotic manipulators," *International Journal of Automation and Computing*, vol. 8, no. 2, pp. 215–220, 2011.

[24] J. Wang and Z. Sun, "6-DOF robust adaptive terminal sliding mode control for spacecraft formation flying," *Acta Astronautica*, vol. 73, pp. 76–87, 2012.

[25] L. Lapierre, D. Soetanto, and A. Pascoal, "Nonlinear Path Following with Applications to the Control of Autonomous Underwater Vehicles," in *Proceedings of the 42nd IEEE Conference on Decision and Control*, pp. 1256–1261, USA, December 2003.

[26] M. Breivik and T. Fossen, "Guidance-Based Path Following for Autonomous Underwater Vehicles," in *Proceedings of the OCEANS 2005 MTS/IEEE*, vol. 3, pp. 2807–2814, Washington, DC, USA, 2005.

[27] T. I. Fossen, *Handbook of marine craft hydrodynamics and motion control*, John Wiley and Sons, 2011.

[28] T. I. Fossen, *Marine Control Systems: Guidance, Navigation and Control of Ships, Rigs and Underwater Vehicles*, Marine Cybernetics, 2002.